

Contaminant Source Identification in Water Distribution Networks: A Bayesian Framework

D. J. Jerez¹, H. A. Jensen^{2,3}, M. Beer^{1,3,4}, and M. Broggi¹

¹*Institute for Risk and Reliability, Leibniz Universität Hannover, 30167 Hannover, Germany.*

²*Department of Civil Engineering, Federico Santa Maria Technical University, Valparaiso, Chile*

³*International Joint Research Center for Engineering Reliability and Stochastic Mechanics, Tongji University, Shanghai 200092, China.*

⁴*Institute for Risk and Uncertainty and School of Engineering, University of Liverpool, Liverpool L69 7ZF, United Kingdom.*

Abstract

This work presents a Bayesian model updating approach for handling contaminant source characterization problems in the context of water distribution networks. The problem is formulated in a Bayesian model class selection framework where each model class represents a possible contaminant event. The parameters of each model class characterize the contaminant mass inflow over time in terms of its intensity and starting time. The class with the highest posterior probability is interpreted as the most plausible location for the contaminant injection. The evidences of the model classes are estimated using the transitional Markov chain Monte Carlo (TMCMC) method. The approach provides additional insight into the current network state in terms of posterior samples of the parameters that describe the contaminant event. The effectiveness of the proposed identification framework is illustrated by applying the contaminant source detection approach to a couple of water distribution systems.

Keywords: Bayesian model updating, Contaminant source identification, Model class selection, Water distribution systems.

1. Introduction

Water distribution networks are constantly exposed to external events that can negatively affect their performance and the safety of the public. One important type of event is the intrusion, accidental or intentional, of contaminants into the system [1, 2]. The presence of an unwanted substance in the network can be very harmful to users and therefore the identification and characterization of any source of contamination is an important goal in water security [3, 4]. In this context, sensor measurements and available system knowledge must be properly taken into account. However, the use of monitoring data in order to identify and characterize the contamination event remains an open challenge in the security of water distribution systems. Relevant attributes of this type of events include the location of the contaminant source, magnitude of the mass inflow, injection starting time, duration, etc. Certainly, the source location is one of the most relevant features since it allows to take corrective actions in a timely manner. Thus, efforts must be directed towards the effective identification of the contaminant source based on available data from an array of sensors located in the network.

Traditionally, the identification of contaminant sources has been treated as a deterministic inverse problem [5, 6]. Direct optimization approaches, particle backtracking algorithm, data mining and machine learning techniques have been reported in this context [7, 8, 9, 10, 11, 12, 13, 14]. The main idea is to determine which contaminant outline can result in simulated sensor measurements that best match the real sensor measurements. One of the difficulties of this type of approaches is the non-uniqueness of the solution to the inverse problem. In fact, due to the nature of the problem, different network characterizations may lead to similar behavior at the measurement points. For instance, responses corresponding to a certain injection point with a given starting time and contamination intensity can be similar to the ones of an upstream point with a higher intensity and an earlier starting time.

Modeling and monitoring processes of water distribution networks involve unavoidable uncertainties in hydraulic engineering practice [15, 16]. These uncertainties must be properly taken into account

when dealing with identification problems in order to improve the overall security and reliability of these critical infrastructure systems [17]. In the context of contaminant source detection, such uncertainties may include sensor noise, nodal demands, modeling errors, attributes of contaminant events, prior knowledge associated with possible source scenarios, etc. To deal with these issues, Bayesian-type of approaches [18] have been also adopted for solving contaminant source characterization problems. The main idea of these approaches is to obtain revised probabilistic information that allows to decide the most plausible contamination source based on available data. Bayesian techniques, in the context of contaminant source detection problems, include the use of factor graph representation and belief propagation [19], beta-binomial conjugate framework coupled with deterministic backtracking algorithms [20], real-time approaches where the posterior information is updated as new measurements become available [21], backward probabilistic modeling [22], and Bayesian belief networks [23, 24]. These methodologies usually identify a region in the network with relatively high plausibility of containing the true sources, and some of them are limited to steady-state hydraulics. An additional type of Bayesian approaches correspond to sample-based model updating techniques [25, 26, 27]. In these contributions, injection location and time profile characteristics are simultaneously considered. Then, a set of posterior samples is obtained and the one that maximizes the posterior probability density function is chosen as the contaminant event. Due to the mixed discrete-continuous nature of the uncertain parameter space, this represents a serious computational challenge in realistic network models. In addition, numerical results reported by the previous contributions have usually identify a broad band of possible sources but they have not been able to single out the true source. Then, it is clear that more research and developments are needed in order to improve the precision, accuracy and efficiency of contaminant source characterization procedures.

In the previous context, this contribution proposes a simulation-based Bayesian model updating framework [28, 29, 30] to deal with contaminant source identification of water distribution systems. In particular, a model class selection problem is formulated where each model class is associated with a potential source location. In this manner, the most probable source locations are selected taking into account all possible contaminant scenarios for any given injection point and therefore

the mixed discrete-continuous nature of the identification parameter space can be circumvented. To solve the model class selection problem a multi-level Markov chain Monte Carlo algorithm, called the transitional Markov chain Monte Carlo (TMCMC) method, is adopted in this work [31]. The method is well-developed and it has been proved in a number of model updating and model class selection applications. Moreover, the approach has been successfully used in resolving some of the difficulties involved in the solution of inverse problems, that is, non-uniqueness, even in presence of limited amount of data and when modeling errors are present. Actually, the TMCMC algorithm can handle globally identifiable cases (set of most probable solutions is a singleton), locally identifiable cases (set of most probable solutions is finite), and unidentifiable cases (set of most probable solutions is uncountable) in an effective manner [31].

Thus, the efforts of this work are focused on the adaptation and implementation of the TMCMC technique into the area of contaminant source characterization with applications to water distribution networks. The approach provides a realistic representation of the uncertainties associated with the hydraulic modeling, water quality behavior, measured data and prior engineering information. The proposed approach is potentially a functional tool for identifying the location of the contaminant sources and estimating the attributes of the contaminant events. In fact, results of the proposed methodology indicate that the location of injection points is clearly identified for practical cases when relatively large model and measurement errors are considered. Thus, the proposed identification process is robust to model and measurement errors for the cases considered in this work. Moreover, the proposed methodology allows to obtain further insight into the contaminant injection profile, in addition to the identification of the contaminant event. This type of information can be useful to assist involved decision making processes in an emergency management framework. The methodology can be considered as an extension of the approach presented in [32] for leakage detection problems.

The organization of the paper is as follows. Section 2 presents the contaminant source identification problem in the framework of Bayesian model updating. The proposed approach is introduced in detail in Section 3. Section 4 discusses some aspects related to the numerical implementation of the proposed method. The effectiveness of the proposed contaminant source identification scheme

is demonstrated in Section 5 by means of two example problems. The paper closes with some conclusions and final remarks.

2. Contaminant Source Identification

2.1. Background and Hypotheses

The presence of unwanted substances in a water distribution network can be very harmful to users and, therefore, it is of the utmost importance to take promptly corrective actions. Once the existence of a contaminant event has been confirmed, it needs to be identified. The existence of contamination can be diagnosed by monitoring the changes in concentration over time at certain control points. Then, the basic idea is to update the hydraulic model in order to identify the location of the contaminant event. In other words, the predictions of the updated hydraulic model will match the measured data obtained from an array of sensors located in the network. Although optimal sensor placement is one of the important aspects of an effective contaminant warning system, this work focuses on source identification with the assumption that sensors are located in the network in a somewhat reasonable, sound, or optimal manner.

To simplify and clarify the demonstration of the proposed approach, the following assumptions are considered in this study. First, the array of sensors provides continuous concentration measurements over time rather than a binary signal indicating the presence or absence of the contaminant. Second, the contamination event is modeled as a constant mass flow entering the network at a single node, that is, the same amount of mass per time unit enters the network at a given node and from a certain time instant. In addition, it is assumed that the contaminant is conservative, i.e., it does not decay as it propagates through the distribution system. Thus, for a given network, the attributes of a contaminant event are determined by three parameters: injection node, contaminant intensity (mass inflow at the injection point), and the starting time. It is noted that, however, multiple sources and alternative injection time profiles can also be considered in the proposed framework. The difference in these cases is that the number of parameters involved in the characterization of the contaminant

events may increase. Finally, the analysis of the water distribution network is carried out using the well known hydraulic simulation program EPANET [33, 34]. In this setting, the hydraulic analysis is based on mass conservation equations at all nodes of the network, and energy conservation equations in all network links. On the other hand, the water quality analysis uses a Lagrangian time-based approach to track discrete parcels of water as they move along pipes and mix together at junctions between fixed-length time steps [33]. However, it is noted that different hydraulic simulation packages can be used as well.

2.2. Contaminant Model Classes

Based on the previous information, the contaminant source characterization requires three network parameters, i.e., the injection node N , the contaminant intensity I , and the starting time T . It is noted that N is a discrete quantity, whereas I and T can be regarded as continuous quantities. Thus, the contaminant source characterization problem presents a mixed discrete-continuous nature in terms of the parameters to be identified, that is, the attributes of a contaminant event. In this framework, it is assumed that N_c network nodes have been identified as potential contaminant injection points. The set $\mathbf{N} = \{1, 2, \dots, N_c\}$ collects the possible injection nodes, that is, $N \in \mathbf{N}$. Clearly, the total number of potential contaminant events N_c is problem-dependent, and it depends on a number of factors such as the layout of the network and additional engineering information. In this regard, appropriate procedures such as particle backtracking algorithms can be used, in principle, to identify the potential contaminant injection points [35, 36]. Since a single contaminant source is assumed, the i^{th} node, $i = 1, 2, \dots, N_c$, is associated with a class of network models, M_i , that comprises all its feasible contaminant injection profiles. This model class is defined by the vector of parameters $\boldsymbol{\theta}_i \in \Theta_i \subset R^2$, with $\boldsymbol{\theta}_i = \{T_i, I_i\}$, where T_i represents the starting time of the contaminant event and I_i represents the mass inflow (contaminant intensity). It is noted that if multiple sources or alternative injection time profiles are considered, the only difference in terms of the present formulation is that the number of model classes or the dimension of the parameter space can increase, as previously pointed out. The parameters $\boldsymbol{\theta}_i$ constitute the set of unknowns

that parametrize the model class M_i . That is, a particular network model $M_i(\boldsymbol{\theta}_i)$ from the class M_i is selected by specifying the values of the parameter set $\boldsymbol{\theta}_i$. In addition, the set of all model classes is defined in the set $\mathbf{M} = \{M_1, \dots, M_{N_c}\}$.

It is noted that when multiple sources of contamination are considered, the injection nodes, contaminant intensities and the starting times constitute the set of attributes of the potential contaminant events. The total number of distinct contaminant events, or model classes, may be quite large in the general case, and therefore an exhaustive search for the most probable events could be computationally very expensive or even prohibitive. In this scenario, stochastic search algorithms [37, 38, 39, 40] can be used to effectively provide a near optimal solution for the injection nodes. In this context, it is important to note that in many practical situations the injection nodes are expected to occur only in a certain number of nodes of the network, and therefore the computational complexity of the problem can be significantly reduced. The consideration of multiple sources of contamination and the corresponding assessment of the proposed methodology is subject for future research (see Conclusions).

3. Proposed Approach

For the purpose of identifying the location of the contamination event, a Bayesian system identification scheme is adopted in this work [41]. The approach is coupled with a hydraulic and water quality behavior simulator for model updating and model class selection of a parametrized class of hydraulic models. It can be regarded as an extension of the methodology introduced in [32, 42] for leakage and connectivity detection problems.

3.1. Model Class Selection

Monitoring data must be gathered and processed to identify the characteristics of the contamination event. The information about the network behavior is denoted by D and it consists of concentration measurements at a number of nodes. The data are used to update the plausibility of all possible

injection nodes, i.e., model classes. The most plausible injection node is obtained by solving a Bayesian model class selection problem [31, 43]. To this end, consider the set $\mathbf{M} = \{M_1, M_2, \dots, M_{N_c}\}$ of the N_c model classes previously defined. Given data D , the posterior probability of each model class, i.e., $P(M_i|\mathbf{M}, D), i = 1, \dots, N_c$ can be determined as

$$P(M_i|\mathbf{M}, D) = \frac{P(D|M_i)P(M_i|\mathbf{M})}{\sum_{l=1}^{N_c} P(D|M_l)P(M_l|\mathbf{M})} \quad (1)$$

where $P(D|M_i)$ is the evidence of the model class M_i , which is a measure of the plausibility of obtaining the measurement data D from M_i . The optimal model class is selected as the one that maximizes $P(M_i|\mathbf{M}, D), i = 1, \dots, N_c$. Each model class has a prior probability $P(M_i|\mathbf{M}), i = 1, \dots, N_c$, which measures the plausibility of contamination occurrence at each node before any information is included into the analysis. For the case where no prior information is available, the prior probabilities can be assumed to be equal, that is, $P(M_i|\mathbf{M}) = 1/N_c$. In this case, the selection among the model classes can be based solely on their evidence values.

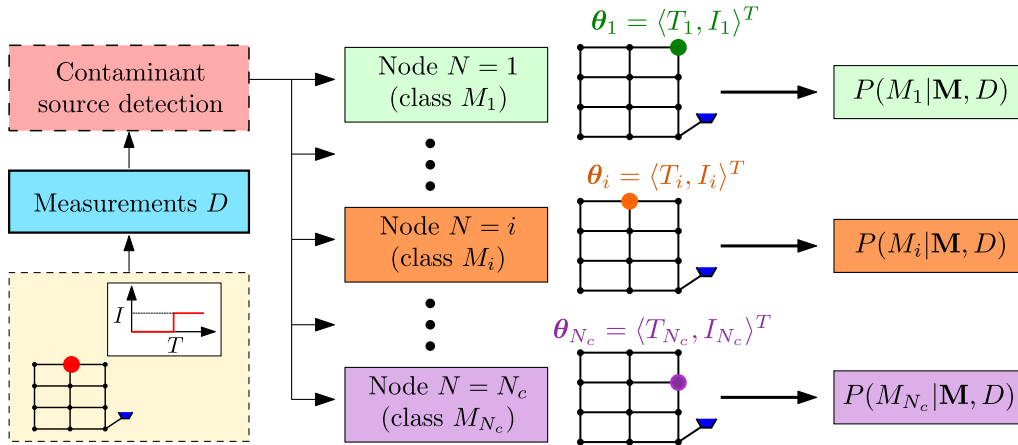


Figure 1: Scheme of the proposed Bayesian model class selection approach

A procedure to estimate the evidence for the different model classes, which involves a Bayesian model updating problem, is addressed in the following sections. For illustration purposes, a sketch of the proposed Bayesian model class selection approach is provided in Figure 1.

3.2. Model Updating

In order to estimate the evidence of a model class, a Bayesian model updating problem is first considered. To this end, the plausibility of each model $M_i(\boldsymbol{\theta}_i)$, within a class M_i , based on concentration measurements D from the network, is quantified by the updated joint probability density function $p(\boldsymbol{\theta}_i|M_i, D)$ (posterior probability density function). According to Bayes' Theorem, the posterior probability density function of $\boldsymbol{\theta}_i$ is given by

$$p(\boldsymbol{\theta}_i|M_i, D) = \frac{p(D|M_i, \boldsymbol{\theta}_i) p(\boldsymbol{\theta}_i|M_i)}{P(D|M_i)} \quad (2)$$

where $p(D|M_i, \boldsymbol{\theta}_i)$ is the likelihood function, $p(\boldsymbol{\theta}_i|M_i)$ is the prior probability density function of $\boldsymbol{\theta}_i$, and $P(D|M_i)$ is the evidence of the model class M_i . The likelihood function expresses the plausibility of observing the data D given a certain $\boldsymbol{\theta}_i$, while the prior probability density function represents the prior or initial belief about the distribution of $\boldsymbol{\theta}_i$. Moreover, the evidence of the model class is written as

$$P(D|M_i) = \int_{\Theta_i} p(D|M_i, \boldsymbol{\theta}_i) p(\boldsymbol{\theta}_i|M_i) d\boldsymbol{\theta}_i \quad (3)$$

where all terms have been previously defined. In the present formulation, a method that estimates the evidence of the model class as a by-product of the solution to the Bayesian model updating problem is implemented. In particular, the transitional Markov chain Monte Carlo (TMCMC) method is adopted [31]. For completeness and clarity, the basic ideas of the TMCMC method are briefly reviewed in the following sections.

3.3. Parameters Estimation

The TMCMC method iteratively proceeds from the prior to the posterior distribution of the parameter set $\boldsymbol{\theta}_i$. To this end, a number of non-normalized intermediate distributions $p_j(\boldsymbol{\theta}_i|M_i, D)$, $j = 0, \dots, m$, are defined as

$$p_j(\boldsymbol{\theta}_i|M_i, D) \propto p(D|M_i, \boldsymbol{\theta}_i)^{\alpha_j} p(\boldsymbol{\theta}_i|M_i) \quad (4)$$

where the parameter α_j increases monotonically with j such that $\alpha_0 = 0$ and $\alpha_m = 1$. The parameter α_j is chosen in such a way that the change of the shape between two adjacent intermediate distributions be small. In this regard, different criteria can be used [31, 44, 45]. This small change of the shape makes it possible to efficiently obtain samples from $p_j(\boldsymbol{\theta}_i|M_i, D)$ based on the samples from the previous distribution. Once the parameter α_j has been computed, the samples at stage j are obtained by generating Markov chains where the lead samples are selected from the distribution $p_{j-1}(\boldsymbol{\theta}_i|M_i, D)$. Each sample of the current stage is generated by applying the Metropolis-Hastings algorithm [46, 47]. The lead sample of the Markov chain is a sample from the previous step, i.e., $\boldsymbol{\theta}_{i,j-1}^k, k = 1, \dots, N_{j-1}$, that is selected according to a probability equal to its normalized weight $\bar{w}(\boldsymbol{\theta}_{i,j-1}^k) = w(\boldsymbol{\theta}_{i,j-1}^k) / \sum_{s=1}^{N_{j-1}} w(\boldsymbol{\theta}_{i,j-1}^s)$, where N_{j-1} is the number of samples at the $j - 1^{th}$ iteration step, and $w(\boldsymbol{\theta}_{i,j-1}^k)$ represents the plausibility weight which is given by $w(\boldsymbol{\theta}_{i,j-1}^k) = p(D|M_i, \boldsymbol{\theta}_{i,j-1}^k)^{\alpha_j - \alpha_{j-1}}$.

The proposal probability density function for the Metropolis-Hastings algorithm is chosen as a Gaussian distribution centered at the lead sample of the chain and with a covariance matrix equal to a scaled version of the estimate covariance matrix of the current intermediate distribution $p_{j-1}(\boldsymbol{\theta}_i|M_i, D)$, that is, $\boldsymbol{\Sigma}_{i,j-1} = \beta^2 \sum_{s=1}^{N_{j-1}} \bar{w}(\boldsymbol{\theta}_{i,j-1}^s) (\boldsymbol{\theta}_{i,j-1}^s - \bar{\boldsymbol{\theta}}_{i,j-1}) (\boldsymbol{\theta}_{i,j-1}^s - \bar{\boldsymbol{\theta}}_{i,j-1})^T$, $\bar{\boldsymbol{\theta}}_{i,j-1} = \sum_{s=1}^{N_{j-1}} \bar{w}(\boldsymbol{\theta}_{i,j-1}^s) \boldsymbol{\theta}_{i,j-1}^s$, where β^2 is a parameter that can be chosen according to different criteria. For example, it can be defined directly by the user or by an adaptive scheme based on the acceptance rate of the sampling process [48, 49]. The procedure is repeated until the parameter α_j is equal to 1 ($j = m$). At the last stage, the samples $\boldsymbol{\theta}_{i,m}^k, k = 1, \dots, N_m$, are asymptotically distributed as $p(\boldsymbol{\theta}_i|M_i, D)$.

3.4. Evidence Estimation

The estimation of the evidences associated with the different model classes is known to be highly nontrivial. In this regard, the TMCMC method provides a flexible and efficient means to estimate

the evidences even in challenging cases such as those involving multi-modal, peaked or flat posterior distributions. In fact, the TMCMC method can estimate the evidences as a by-product and they are given in terms of the mean values of the weights at the different stages, $W_{i,j} = \sum_{k=1}^{N_j} w(\boldsymbol{\theta}_{i,j}^k) / N_j$, as

$$W_i = \prod_{j=0}^{m-1} W_{i,j} \quad (5)$$

where W_i is an asymptotically unbiased estimator of the evidence $P(D|M_i)$ [31]. Note that if only the evidences are required, the process can be stopped at stage $j = m - 1$. The reader is referred to [31, 48] for a detailed description of the TMCMC method. A pseudo-code that illustrates the implementation of the TMCMC method is provided in the Appendix.

4. Implementation Aspects

4.1. Contaminant Data

The likelihood function, $p(D|M_i, \boldsymbol{\theta}_i)$, which measures how plausible is to obtain measurements D from each model $M_i(\boldsymbol{\theta}_i)$ is defined as follows. In the context of the present formulation, it is assumed that the data D are obtained from n_S sensors at n_T time instants. Then, the concentration measurements are contained in a vector $\mathbf{y} \in R^{n_S \times n_T}$ where $\mathbf{y} = \langle \mathbf{y}_1^T, \dots, \mathbf{y}_{n_S}^T \rangle^T$, in which $\mathbf{y}_j \in R^{n_T}$, $j = 1, \dots, n_S$ is a vector comprising the measurements at the j^{th} sensor and given by $\mathbf{y}_j = \langle y_j(t_1), \dots, y_j(t_{n_T}) \rangle^T$, where $y_j(t_k)$ represents the concentration level at the j^{th} sensor location at time instant t_k , $k = 1, \dots, n_T$. Formally, the prediction errors from the model $M_i(\boldsymbol{\theta}_i)$ are written as $e_{jk}(\boldsymbol{\theta}_i) = y_j(t_k) - y_j(t_k, \boldsymbol{\theta}_i)$, $j = 1, \dots, n_S$, $k = 1, \dots, n_T$, where $y_j(t_k, \boldsymbol{\theta}_i)$ indicates the concentration level at the j^{th} sensor location at time instant t_k computed from the model class M_i , corresponding to a particular value assigned to the parameter set $\boldsymbol{\theta}_i$. The prediction errors may be due to hydraulic and water quality behavior network modeling and device measurement accuracy that are unavoidable in the modeling and monitoring processes of real water distribution systems, and they are modeled as normally distributed with zero mean and covariance matrix \mathbf{C} . Based on the previous conditions, the likelihood function $p(D|M_i, \boldsymbol{\theta}_i)$

is written as [28, 29, 50]

$$p(D|M_i, \boldsymbol{\theta}_i) \propto |\mathbf{C}|^{-1/2} \exp \left[-\frac{1}{2} L(\boldsymbol{\theta}_i, \mathbf{y}) \right] \quad (6)$$

where \propto indicates proportional, $|\cdot|$ denotes determinant, and $L(\boldsymbol{\theta}_i, \mathbf{y})$ is a weighted measure of fit between the model predictions and the measured data given by

$$L(\boldsymbol{\theta}_i, \mathbf{y}) = [\mathbf{y} - \mathbf{y}(\boldsymbol{\theta}_i)]^T \mathbf{C}^{-1} [\mathbf{y} - \mathbf{y}(\boldsymbol{\theta}_i)] \quad (7)$$

where $\mathbf{y}(\boldsymbol{\theta}_i)$ represents the corresponding vector of measurements computed from the model class $M_i(\boldsymbol{\theta}_i)$. For simplicity, the prediction errors are assumed to be independent and, therefore, the covariance matrix \mathbf{C} is a diagonal matrix comprising the prediction error variances. It is noted that, however, different prediction error model classes can be used as well, including models that consider correlation [51, 52]. Finally, it is noted that, in the framework of model updating, parameters associated with the characterization of the covariance matrix can also be included in the parameter set $\boldsymbol{\theta}_i$.

4.2. Hydraulic and Water Quality Simulation Model

The widely used software EPANET 2.2 is employed in this work for analysis purposes [33, 34]. In other words, measurements computed from the model classes, in the framework of the TMCMC method, are generated by this algorithm. The software allows performing extended period simulation of hydraulic and water quality behavior of water distribution networks. Hydraulic analysis is based on mass conservation equations at all nodes of the network (pipe connection points, tanks and reservoirs), and energy conservation equations in all network links (pipes, pumps and valves). These two types of relationships lead to a system of nonlinear equations that is solved using a type of Newton iteration scheme. On the other hand, water quality analysis, which simulates the concentration over time of different substances in all network components, uses a Lagrangian time-based approach to track

discrete parcels of water as they move along pipes and mix together at junctions between fixed-length time steps [33]. Water quality analysis uses information gathered from a previous hydraulic simulation of the network in order to propagate the substance across the network. Hence, water quality results do not affect the hydraulic behavior of the system under analysis. Validation calculations have shown the efficiency and flexibility of this simulation model in a large number of water distribution networks.

4.3. Computational Efficiency

The proposed approach presents several advantages for implementation in a high-performance computing (HPC) environment. In fact, all model classes are perfectly independent from each other. Thus, the estimation of the evidences of the different model classes is perfectly parallel and the analyses can be carried out simultaneously taking advantage of available parallelization techniques. Moreover, the first stage of the TMCMC method corresponds to direct Monte Carlo simulation and, therefore, it can be completely scheduled in parallel. In addition, subsequent stages involve the generation of a number of Markov chains that are perfectly parallel. Hence, the corresponding sampling process can also be scheduled in a parallel setting. The load balance in the computer workers can be based on a static or dynamic job-scheduling scheme [53]. Clearly, if a high-performance computing environment is not available, the evidences for each potential contaminant event need to be estimated in a sequential manner. Although such estimation may be computationally expensive and could represent a possible limitation of the methodology, in many practical situations the injection nodes are expected to occur only in a certain number of nodes of the network. For instance, available pre-screening techniques [35, 36] as well as engineering knowledge about the network can be used to rule out unfeasible nodes before the identification process is carried out. In addition, surrogate models can be integrated, in principle, to reduce the computational efforts associated with the evaluation of the likelihood function [49, 50]. Thus, the computational complexity of the problem can be significantly reduced, even for the case when a HPC environment is not accessible. The implementation and evaluation of the previous techniques within the proposed approach represent a future research effort.

5. Numerical Examples

5.1. Simplified Network Model

The objective of this example is to study in detail some of the capabilities of the proposed contaminant source identification scheme. In particular, the effect of increasing the amount of available data and the effect of model and measurement uncertainties on the performance of the approach are explored. To this end, two cases are analysed in terms of the uncertainty included in the identification process. Case A considers uncertainty in the hydraulic model properties, whereas case B considers both, modeling and measurement errors. In addition, two scenarios in terms of the amount of measurements are studied in each case.

5.1.1. Network Description

A simple network subject to a contamination event is considered in the test problem. The network is shown in Figure 2 and comprises 17 nodes, 21 pipes and a single reservoir. The distances between the nodes are also indicated in the figure. All nodes are located at the same level, whereas the reservoir has a relative height of 15 m. The water enters to the distribution system through node 1. The head-losses in pipes are modeled using the Darcy-Weisbach equation. All pipes are of diameter 110 mm, with roughness coefficient $\varepsilon = 0.0046$ mm. The nodes have a maximum demand of 0.5 l/s and follow a typical demand pattern which is shown in Figure 3. An extended period of 36 hours is shown in the figure.

For illustration purposes, it is assumed that the injection point is node 1, as indicated in Figure 2. The substance can propagate to all network nodes and a periodic behavior of the contaminant concentration response can be eventually reached at every point of the network. The injection of the substance starts two hours after the beginning of the simulation period. A constant intensity of 100 mg/min is considered. The hydraulic and water quality time step, in the context of EPANET, is 5 min.

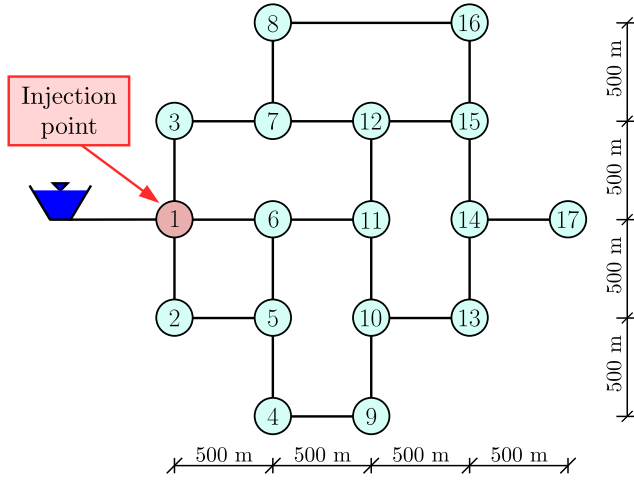


Figure 2: Water distribution network. Test problem

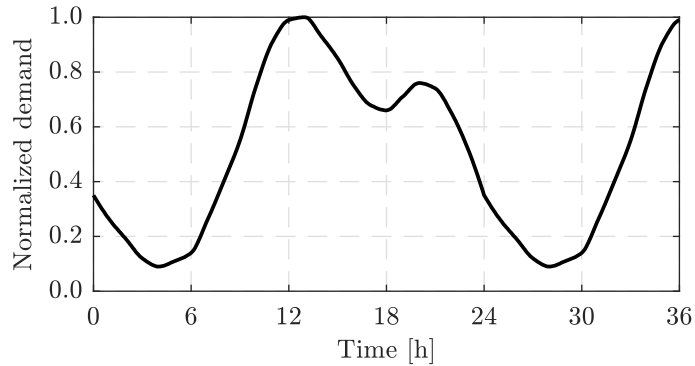


Figure 3: Normalized demand pattern

5.1.2. Synthetic Measurements

The performance of the proposed identification process is evaluated considering synthetic measurements. The data considered for identification purposes are concentration levels over time obtained at nodes 10 and 17, whose location is shown in Figure 4. The corresponding time history of the contaminant injection is also shown in the figure. As previously mentioned, continuous-valued sensors are considered for the identification process. Measurement and modeling errors are accounted explicitly in the analysis in order to consider a realistic setting [32, 42, 54]. In order to include measurement noise in the sensors, an error term is added to the predictions of the actual network. Simulated data are generated as

$$y_j(t_k) = y_j^{\text{actual}}(t_k) + y_j^{\text{noise}}(t_k), \quad j = 1, \dots, n_S, \quad k = 1, \dots, n_T \quad (8)$$

where $y_j^{\text{actual}}(t_k)$ represents the concentration level in the actual system and $y_j^{\text{noise}}(t_k)$ accounts for the measurement error. The quantities $y_j^{\text{actual}}(t_k)$ are obtained from an EPANET model that is representative of the actual system and it is referred to as the actual network. This model has hydraulic properties that deviate from the ones considered for identification purposes. The particular characteristics that are perturbed from their nominal values are the pipe roughness coefficients and peak nodal demands. The roughness coefficient of the l^{th} pipe at the actual network is given by $\varepsilon_l^{\text{actual}} = \varepsilon_l^{\text{nominal}}(1 + \alpha u_l)$, where $\varepsilon_l^{\text{nominal}}$ is the roughness coefficient of the l^{th} pipe in the model class used for identification, u_l is a random number uniformly distributed over $[-1, 1]$ and $\alpha \in [0, 1]$ represents the intensity of the uncertainty expressed as a percentage of the nominal value. Similarly, the peak demand of the l^{th} node is written as $\delta_l^{\text{actual}} = \delta_l^{\text{nominal}}(1 + \beta u_l)$, where $\delta_l^{\text{nominal}}$ is the peak demand of the l^{th} node in the model class used for identification, u_l is a random number uniformly distributed over $[-1, 1]$ and $\beta \in [0, 1]$ represents the intensity of the uncertainty expressed as a percentage of the nominal value. Thus, it is clear that the model classes used for identification are not capable to represent the behavior of the actual network exactly.

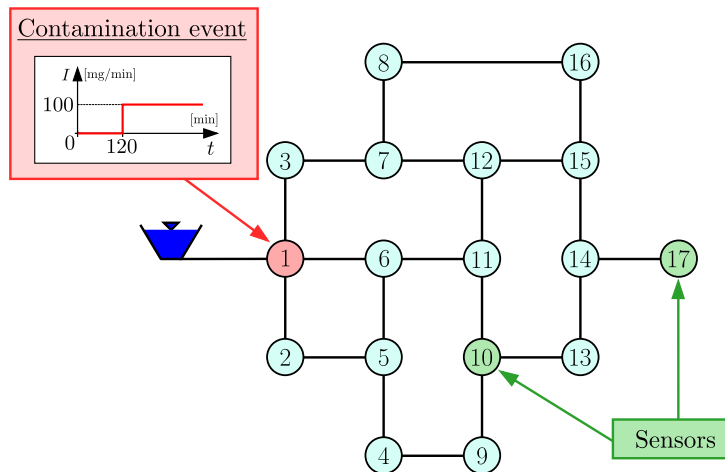


Figure 4: Location of sensors in the network

Moreover, the measurement error $y_j^{\text{noise}}(t_k)$ is generated as $y_j^{\text{noise}}(t_k) = y_j^{\text{actual}}(t_k) \gamma u_{j,k}$, where $u_{j,k}$ is

a random number uniformly distributed over $[-1, 1]$ and $\gamma \in [0, 1]$ represents the measurement noise intensity expressed as a percentage of the response obtained from the actual network.

5.1.3. Definition of Probabilistic Model Classes

The set of probabilistic model classes comprises all feasible contaminant source locations based on prior engineering information. All network nodes are considered as potential injection points with the same plausibility. Thus, the posterior probability of $N_c = 17$ model classes must be evaluated. As previously pointed out, appropriate techniques such as particle backtracking algorithms can be used, in principle, to reduce the number of potential contaminant injection points [35, 36]. As discussed in Section 2, each model class involves a constant mass flow into a given node starting at a given time instant. Hence, the i^{th} model class, M_i , is parametrized by $\theta_i = \langle T_i, I_i \rangle^T$, where T_i is the injection's starting time and I_i is the contaminant intensity. A uniform prior distribution for the uncertain parameters θ_i is considered for each model class. They are defined in the intervals $T_i \in [0, 540]$ min, and $I_i \in [0, 1000]$ mg/min. The upper bound for the starting time is associated with the first arrival of the contaminant to the sensors.

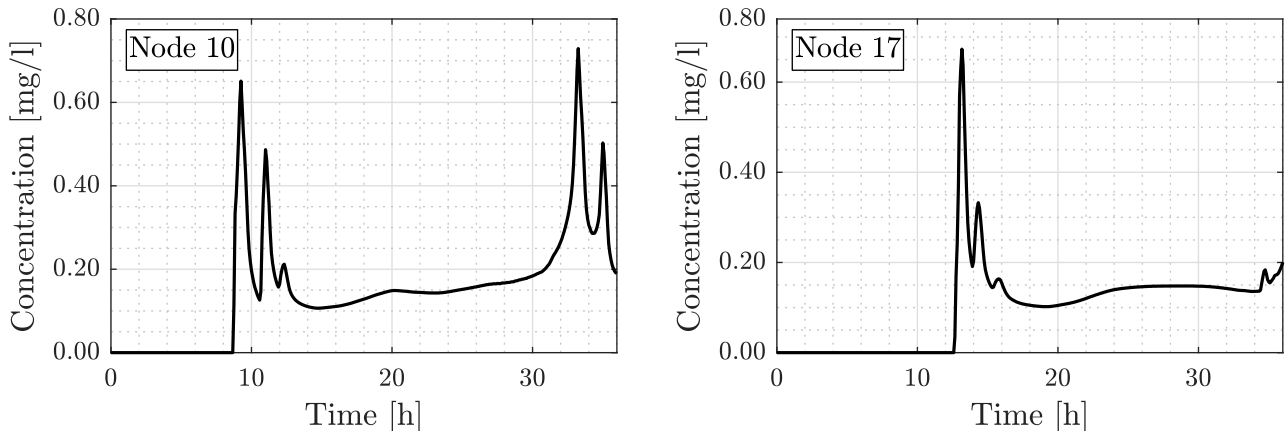


Figure 5: Measurements of nodal concentration over time. Idealized network

In this regard, Figure 5 shows the measurements obtained at the sensors when no errors are considered in the analysis, that is, $\alpha = \beta = \gamma = 0$ (idealized network). It can be observed that the contaminant arrives at node 10 about seven hours after the injection starts. On the other hand, the contaminant

arrives at node 17 about ten hours after the start of the injection. Then, it is observed that the source start time can be anytime from 9 hours before the time of first detection up to the time of detection. Similar arrival times are obtained when model and measurement uncertainties are considered. Based on the previous information, the upper bound of the starting time is set equal to 540 min (9 hours). For reference purposes, recall that the actual contaminant source location is node 1, with starting time $T_1 = 120$ min, and intensity $I_1 = 100$ mg/min. In terms of the TMCMC method, 100 samples per stage are considered in its implementation.

5.1.4. Results of Case A: Hydraulic Model Uncertainty

Model errors are imposed by perturbing the values of all pipe roughness coefficients and peak nodal demands, as previously pointed out. For illustration purposes, relatively large perturbations are introduced simultaneously for the pipe roughness coefficients and peak nodal demands. In particular, $\alpha = \beta = 10\%$. In terms of the proposed framework, it is assumed that all probabilistic model classes present the same prior probability, since there is no particular preference to any possible injection node based on previous information. Then, the model class selection problem can be addressed considering only the evidence values. In addition, two scenarios are considered regarding the dataset size used in the analysis. The first scenario considers measurements up to the time of first detection of the contaminant (5 min after the first detection), while the second scenario contemplates measurements up to 60 min after the first arrival of the contaminant to any sensor (about 10 hours).

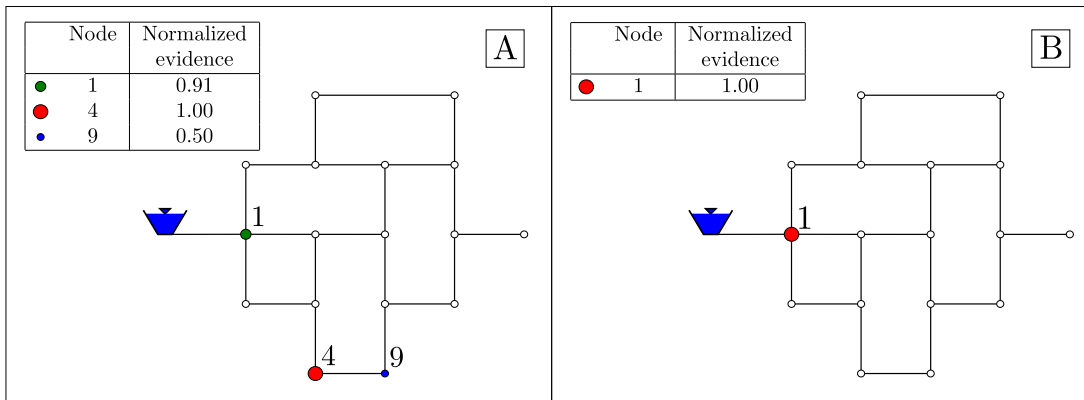


Figure 6: Normalized evidences of all model classes. A) Scenario 1. B) Scenario 2. Hydraulic model uncertainty

Figure 6 shows the normalized evidences of the model classes associated with the different injection nodes obtained for both scenarios. The normalized evidences are such that their maximum value is equal to one. It is observed that the injection node is correctly identified in the second scenario (Figure 6-B), where the normalized evidence of model class 1, which considers node 1 as the injection point, is equal to one, and the evidences of the other model classes are almost equal to zero. However, the actual injection node is not identified correctly in the first scenario (Figure 6-A). In fact, the most probable contaminant event identified corresponds to injection node 4. Additionally, contaminant injection in nodes 1 and 9 also leads to model classes with evidences different to zero. It is noted that nodes 1, 4 and 9 are upstream from node 10, which is consistent from the physical point of view. Thus, although the actual injection node is not identified correctly, the results still provide important information about the network behavior. When more data are available, the contaminant event is properly determined as indicated from the results associated with Scenario 2, where the location of the injection point is clearly identified even when relatively large model errors are included in the model that generates the data.

To obtain further insight into the contaminant source identification process, Figure 7 shows the corresponding identification process when using model class M_1 , that is, the most probable model class. This figure shows how the samples in the $T_1 - I_1$ space converge for the actual contaminant event during the different TMCMC stages when the second scenario is considered. Note that both, the contaminant intensity and the starting time are correctly identified. The starting time ranges from 120 to 135 min, whereas the contaminant intensity values range from 97.3 to 112.0 mg/min. The posterior mean estimate of the model parameters is $\theta_1 = \langle T_1, I_1 \rangle^T = \langle 124.9, 104.1 \rangle^T$. From the different steps of the identification process, it is clear that the prior uncertainty of the contaminant intensity value and the starting time is significantly reduced due to the available data.

5.1.5. Results of Case B: Hydraulic Model and Measurement Errors

To consider a more practical and realistic situation, it is assumed that model and measurement errors are present in the analysis. To this end, the perturbation levels for the pipe roughness coefficients,

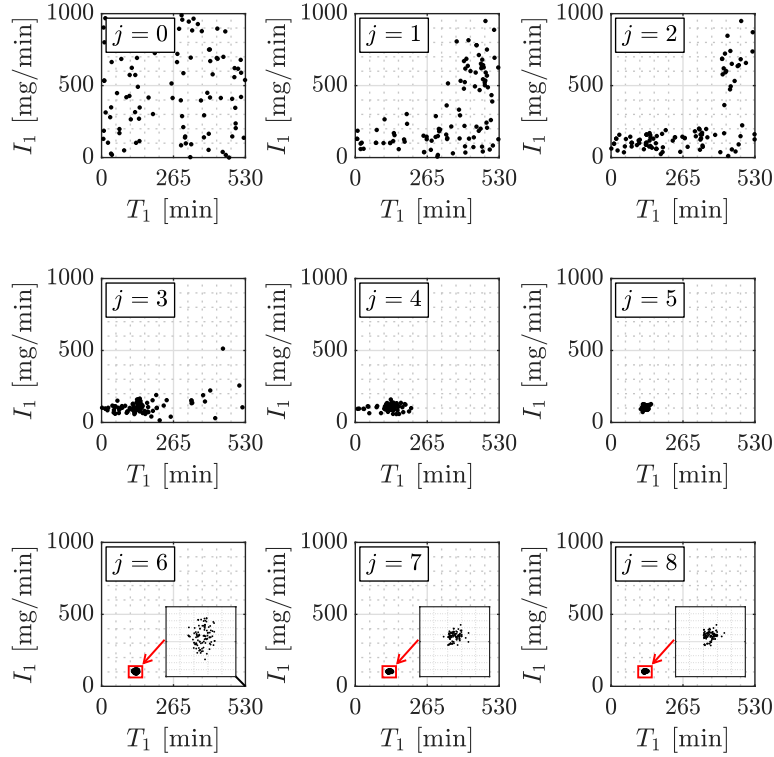


Figure 7: Plot of samples in the $T_1 - I_1$ space generated at different steps of the transitional Markov chain Monte Carlo method when updating model class M_1 . Hydraulic model uncertainties

peak nodal demands, and measurement noise intensities are taken equal to $\alpha = \beta = \gamma = 10\%$. Figure 8 shows the normalized evidences obtained for scenarios 1 and 2. Under this case, the actual contaminant event is not correctly identified in the first scenario (Figure 8-A), but the most probable injection points are located across the flow paths from the actual injection location (node 1) to the sensor recording non-zero concentrations (node 10), as in Case A where only model uncertainties are considered. Thus, although the correct node is not identified, the proposed approach still provides relevant information about the current state of the network.

If more information is available, i.e., Scenario 2 (Figure 8-B), the injection node is properly determined. In fact, among all model classes, the proposed identification scheme clearly favors model class M_1 . Thus, it is clear that increasing the amount of available data is highly beneficial towards the identification process, which is reasonable from the practical point of view. The corresponding identification process when using model class M_1 is shown in Figure 10. This figure shows the evo-

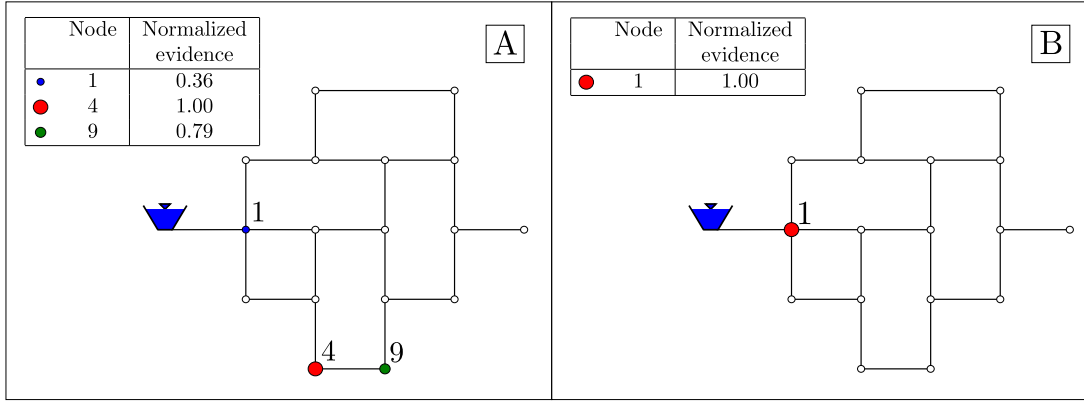


Figure 8: Normalized evidences of all model classes. A) Scenario 1. B) Scenario 2. Hydraulic model and measurement errors

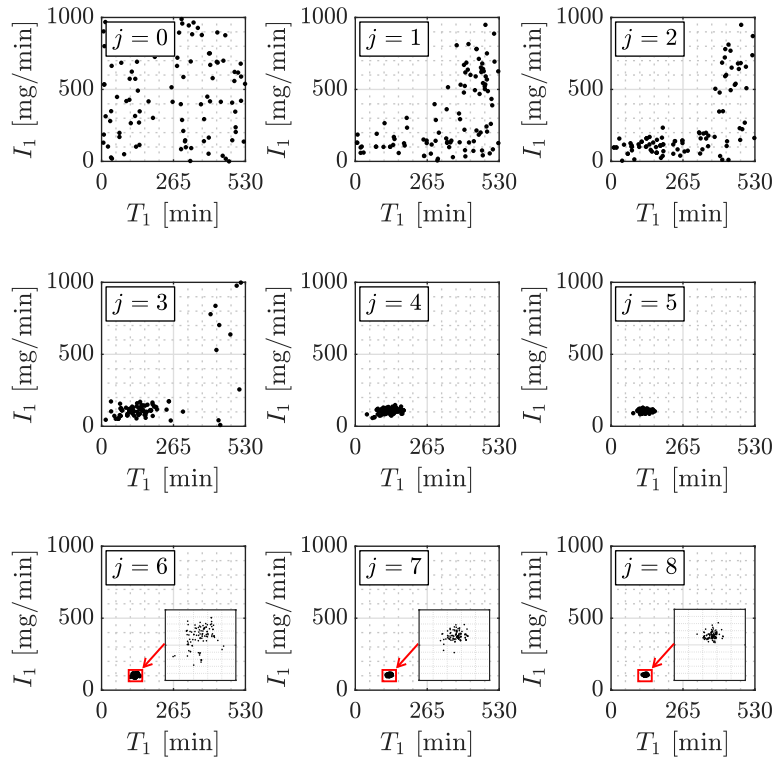


Figure 9: Plot of samples in the $T_1 - I_1$ space generated at different steps of the transitional Markov chain Monte Carlo method when updating model class M_1 . Hydraulic model and measurement errors

lution of samples in the $T_1 - I_1$ space during the different TMCMC stages. At the final stage of the identification process, the starting time ranges from 116 to 134 min, whereas the contaminant intensity values range from 101.6 to 115.5 mg/min. The posterior mean estimate of the model parameters is $\theta_1 = \langle T_1, I_1 \rangle^T = \langle 126.4, 106.6 \rangle^T$. Then, the samples of the model parameters θ_1 are distributed around the actual value, as for the case where only model uncertainties are considered. Note that

the model parameters (contaminant intensity and starting time) are globally identifiable since the set of posterior samples (most probable model parameters) populates a vicinity of the target values. Based on the previous results, it is concluded that the identification of the contaminant event is quite robust to model and measurement errors for this particular network.

5.2. Application Problem

The objective of this example is to evaluate the capabilities of the proposed approach in a more realistic network model. Two different events are considered in terms of the location of the contaminant source. For each event, two different scenarios in terms of the amount of measurements are contemplated. In all cases, modeling and measurement uncertainties are included in the data generation process.

5.2.1. Description of the Network

The water distribution network considered as an application problem corresponds to Example Network 3 provided as a tutorial in EPANET 2.2 [33]. This system has been studied in the context of contaminant source detection by other researchers in previous contributions [20, 21, 25, 26, 27]. It consists of 92 nodes, 117 pipes, two reservoirs, three fully-mixed tanks and two pumps. The layout of the network and some of its elements are shown in Figure 10. Transient flows are developed in the pipeline system due to the varying operational conditions, demand requirements, and the filling and draining of the storage tanks during the network operation. In this context, most nodes follow the normalized demand pattern shown in Figure 11 during the analysis period. In addition, a total of 65.75 km of pipelines are allocated to distribute water to the different nodes. The pipe distributions in terms of Hazen-Williams coefficients and diameters are shown in Tables 1 and 2, respectively. A simulation period of 24 h is considered for analysis purposes. The corresponding hydraulic simulation step and water quality step are equal to 5 min.

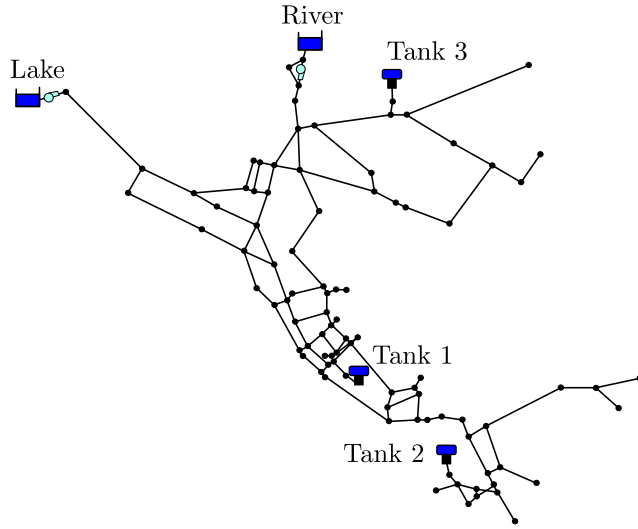


Figure 10: Water distribution network. Application problem

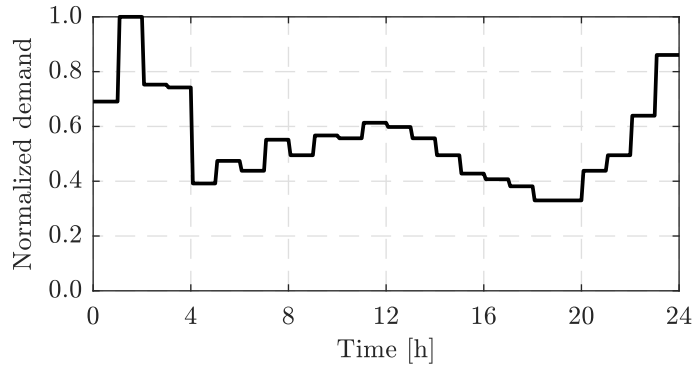


Figure 11: Normalized demand pattern. Application problem

Hazen-Williams coefficient	Number of pipes	Total length (km)
110	1	4.33
130	97	41.40
140	4	14.24
141	12	5.69
199	3	0.09

Table 1: Distribution of pipes in terms of their roughness coefficients. Application problem

5.2.2. Contamination events

Two different contamination events are studied in order to explore the capabilities of the proposed approach. In each event, a conservative chemical is injected at a single node with a constant mass inflow of 0.2 kg/min. The location of these two events within the network is illustrated in Figure 12.

Diameter (mm)	Number of pipes	Total length (km)
203.2	25	10.97
254.0	4	1.18
304.8	50	20.22
355.6	3	0.82
406.4	7	6.07
457.2	1	4.33
508.0	1	0.24
609.6	10	3.69
762.0	13	18.15
2514.6	3	0.09

Table 2: Distribution of pipes in terms of their diameters. Application problem

Event 1 is associated with a contaminant inflow at node 101, starting 2 h after the beginning of the simulation. On the other hand, Event 2 corresponds to a contaminant injection into node 157, starting 5 h after the beginning of the simulation. Note that compared with Event 1, a more complex contaminant propagation pattern can be expected in Event 2 since node 157 is located in an intermediate sector of the network. The attributes of each event under consideration are summarized in Table 3.

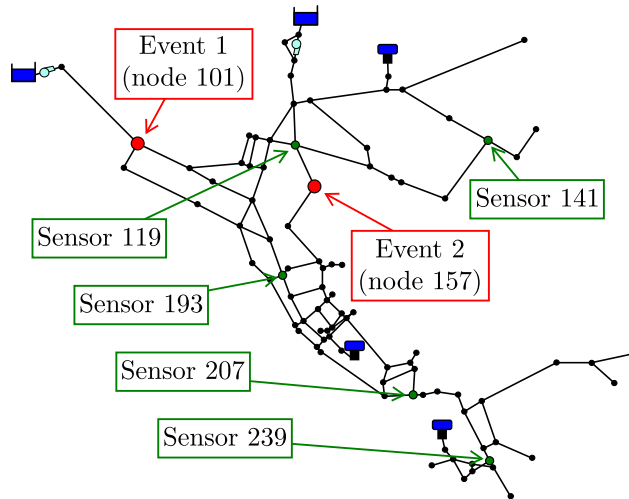


Figure 12: Location of contaminant sources and array of sensors. Application problem

Concentration measurements at given network nodes are considered for identification purposes. In this context, five fixed sensors recording contaminant concentration every 5 min are allocated in the network according to Figure 12. This array of measuring devices is the one reported in [20], which

is based on the example provided in the threat ensemble vulnerability assessment and sensor placement optimization tool (TEVA-SPOT) toolkit [20, 55]. The same sensor configuration is considered for both contaminant events. Finally, the corresponding concentration measurements are obtained according to Section 5.1.2. Modeling and measurement uncertainties have been simultaneously considered in the data generation processes for both events. In this manner, a more realistic scenario in terms of the available information about the actual network condition is addressed. As in the test problem, 100 samples per stage are considered in the framework of the TMCMC method.

	Event 1	Event 2
Source node	101	157
Intensity I (kg/min)	0.2	0.2
Starting time T (min)	120.0	300.0

Table 3: Attributes of the contaminant events. Application problem

5.2.3. Results: Event 1

This event is associated with a contaminant injection at node 101, that is, close to one of the water sources (see Figure 12). For illustration purposes, Figure 13 shows the corresponding concentration measurements at the sensors during the entire simulation period when no uncertainties are taken into account, that is, $\alpha = \beta = \gamma = 0$. It is noted that the contaminant arrives first to node 193 about 60 min after the injection starts, and the concentrations tend to decrease at the end of the analysis period. This is attributed to the varying operational conditions of the system under analysis. For reference purposes, the actual values of the contamination parameters for Event 1 are $T = 120$ min and $I = 0.2$ kg/min.

The synthetic measurements considered for identification purposes are obtained considering model and measurement errors as previously pointed out. In particular, the uncertainty levels are given by $\alpha = \beta = \gamma = 10\%$. The Bayesian model class selection problem considers all network nodes as potential injection points with the same degree of plausibility. This leads to a total of $N_c = 92$ model classes whose posterior probability needs to be estimated. The parameters of each model class M_i are given by $\theta_i = \langle T_i, I_i \rangle^T$ where T_i is the injection's starting time and I_i is the constant mass inflow

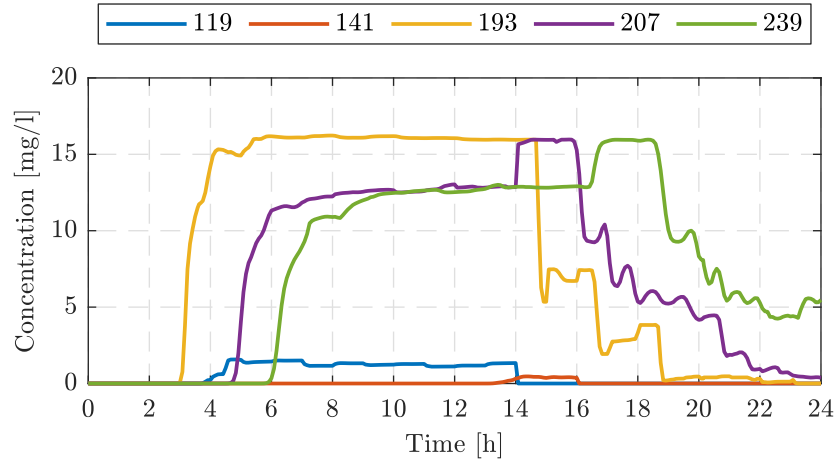


Figure 13: Measurements of nodal concentration over time. Application problem. Event 1

(contaminant intensity). The prior distribution for the model parameters is taken as uniform with $I_i \in [0, 1]$ kg/min and $T_i \in [0, 180]$ min. It is noted that the upper bound for the starting time corresponds to the instant in which the contaminant arrives to the sensors for the first time.

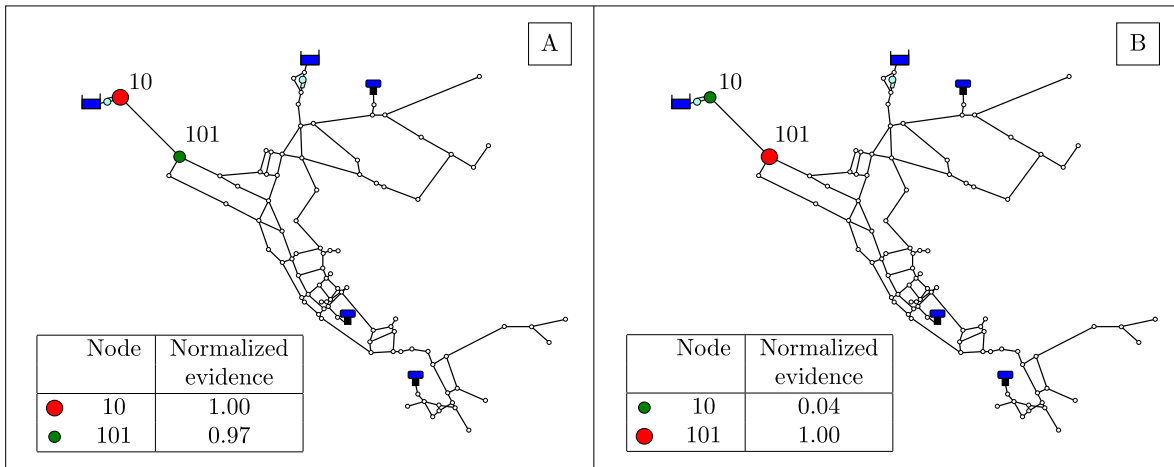


Figure 14: Normalized evidences of all model classes. Application problem. Event 1. A) Scenario 1. B) Scenario 2

The contaminant source characterization process is carried out considering two cases in terms of the amount of available measurements. Scenario 1 considers measurements from the beginning of the simulation up to 60 min after the contaminant arrives to two sensors (about 5 hours), whereas Scenario 2 considers measurements during the entire analysis period (24 hours). Since all injection points have the same prior probability, the model class selection process can be performed solely based on their evidences. Figure 14 illustrates the normalized evidences obtained for all model classes,

where nodes with normalized evidence close to zero have been depicted with small white circles. For Scenario 1 (see Figure 14-A), two nodes have similar evidence values. In fact, the evidence of node 10 is slightly larger than of the actual contamination source (node 101). Validation calculations show similar results when considering measurements up to 60 min after the initial contaminant detection (about 4 hours). It is observed that nodes 10 and 110 are adjacent, that is, they belong to the same pipeline. Thus, even when the actual injection point is not identified as the most probable one, the results still provide information that can be useful to decision makers. When the measured data consider the entire simulation period, i.e., Scenario 2, (see Figure 14-B), the actual injection point is properly identified. Moreover, the evidence of node 10 represents about 4% of the evidence of node 101 in this case. This illustrates that the system identifiability seems to improve as the amount of available measurements increases.

The proposed methodology can provide additional insight into the contaminant event in terms of posterior samples of the model parameters. To illustrate this, Figure 15 shows the evolution of samples obtained during the different stages of the TMCMC method when Scenario 2 is considered. It is noted how the samples converge from the prior distribution (stage $j = 0$) to the posterior distribution (stage $j = 10$). The posterior samples are concentrated near the actual values for the contamination parameters. Thus, the model parameters are globally identifiable in this case. At the last stage, the starting time ranges from 125 to 130 min, while the contaminant intensity from 0.201 to 0.204 kg/min. The corresponding posterior mean estimate of the model parameters is given by $\boldsymbol{\theta} = \langle T, I \rangle^T = \langle 127.3, 0.203 \rangle^T$. The slight differences with respect to the target values are explained due to the presence of measurement noise and modeling errors. Note that, however, these values can be considered as the actual values from a practical point of view.

5.2.4. Results: Event 2

The contaminant is injected at node 157 in this event. This node is located in an intermediate sector of the network (see Figure 12). The corresponding target values of the contaminant source parameters are $T = 300$ min for the starting time and $I = 0.2$ kg/min for the contaminant intensity. The

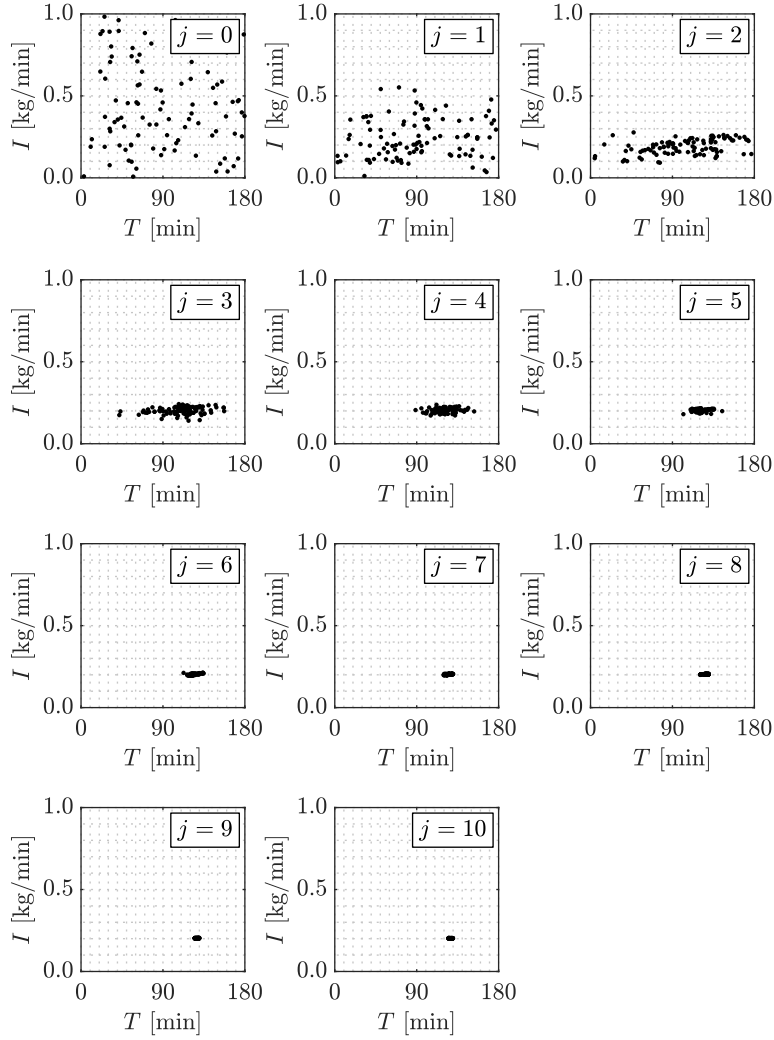


Figure 15: Plot of samples in the $T - I$ space generated at different steps of the transitional Markov chain Monte Carlo method when updating the model class associated with node 101. Application problem. Event 1

concentration measurements reported in Figure 16 are associated with Event 2 when no uncertainties are taken into account, i.e., $\alpha = \beta = \gamma = 0$. In this case, the contaminant arrives first to sensor 207 after 135 min of continuous injection, that is, 435 min since the beginning of the simulation period. On the other hand, sensors 119 and 141 do not receive contaminant influence during that period of time. This is attributed to the location of the contaminant source as well as to the flow patterns developed during the simulation period.

Model and measurement uncertainties are considered in this event. The uncertainty levels in roughness coefficients, peak nodal demands and concentration measurements are given by $\alpha = \beta = \gamma =$

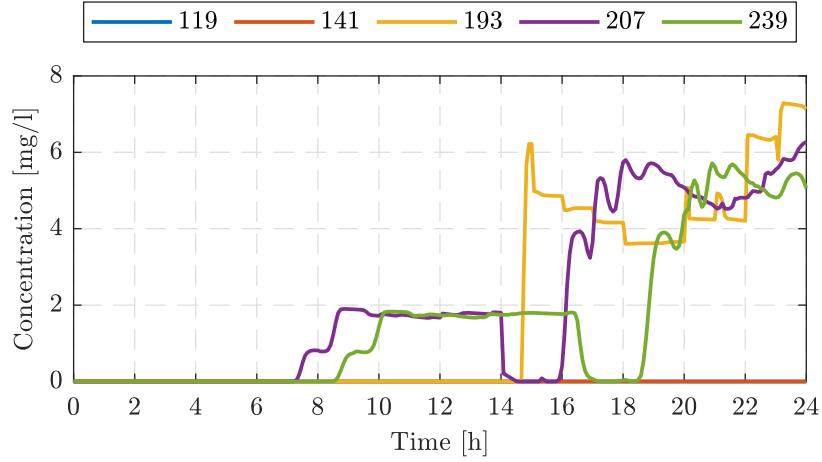


Figure 16: Measurements of nodal concentration over time. Application problem. Event 2

10%. As for the previous event, $N_c = 92$ model classes are considered with parameters $\theta_i = \langle T_i, I_i \rangle^T$ for each model class. A uniform prior distribution is considered with $I_i \in [0, 1]$ kg/min and $T_i \in [0, 435]$ min. The upper limit for T_i coincides with the arrival time of the contaminant to the sensors.

Two scenarios in terms of the time-span for measurements are addressed, as in Event 1. Scenario 1 involves measurements from the beginning of the simulation up to 60 min after the contaminant arrives to two sensors (about 10 hours), whereas Scenario 2 considers measurements over the entire simulation period (24 hours). As in the previous event, the source identification can be performed based on the evidence values only. In this context, Figure 17 presents the normalized evidences of all potential injection locations. Normalized evidences close to zero are depicted with small white circles. It is seen that only node 195 presents a normalized evidence different from zero in Scenario 1 (see Figure 17-A), that is, the contaminant source is not properly identified when considering measurements up to 60 min after the detection in a second sensor. On the other hand, the identification results improve when more data are incorporated in the identification process. In fact, the actual contamination source (node 157) is identified as the most plausible in Scenario 2 (see Figure 17-B), although nodes 159 and 161 present similar evidence values. It is noted that validation calculations show similar results when considering measurements up to 60 min after the contaminant arrives to three sensors (about 16 hours). These results are reasonable from the hydraulic viewpoint

since these three nodes are part of a single flow path and, therefore, contaminant injection in any of these locations generates similar propagation patterns through the water distribution network.

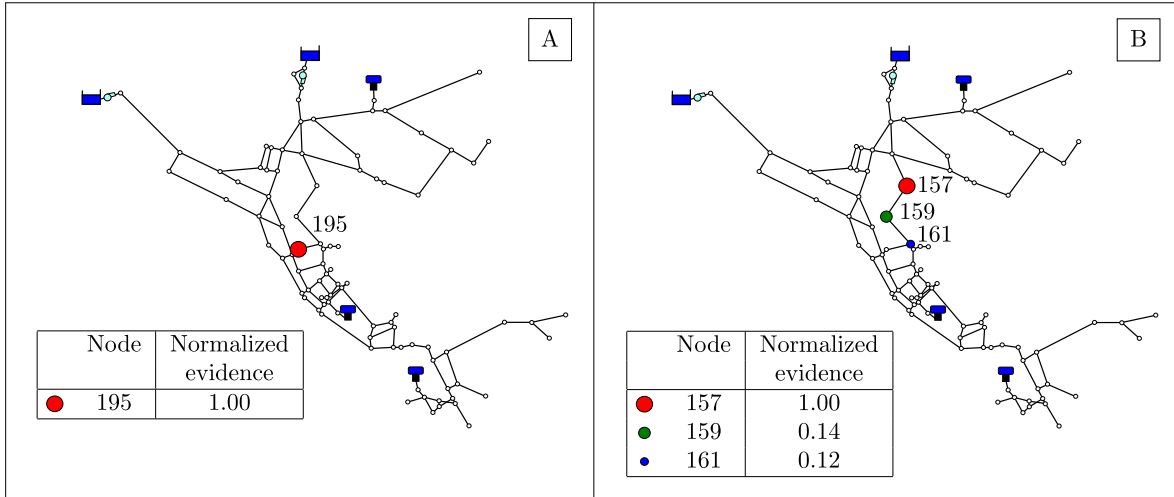


Figure 17: Normalized evidences of all model classes. Application problem. Event 2. A) Scenario 1. B) Scenario 2

Figure 18 shows the samples obtained during the different stages of the TMCMC method for the model class associated with node 157 and considering measurements over the entire simulation period. The samples at the initial stage ($j = 0$) are drawn from the prior distribution whereas the last stage ($j = 7$) generates samples from the posterior distribution. It is seen how measurement data significantly reduce the uncertainty in the model parameters. Note that the posterior samples populate a vicinity of the target values for the model parameters, and therefore the model parameters are globally identifiable as in Event 1. In fact, the starting time ranges from 279.8 to 311.4 min and the contaminant intensity from 0.198 to 0.207 kg/min at the last stage. Moreover, the corresponding posterior mean estimate is $\theta = \langle T, I \rangle^T = \langle 297.7, 0.203 \rangle^T$. These results illustrate one of the advantages of the proposed methodology, which allows to obtain further insight into the contaminant injection profile in addition to the solution to the model class selection problem. This type of information can be potentially useful to assist involved decision making processes in an emergency management framework.

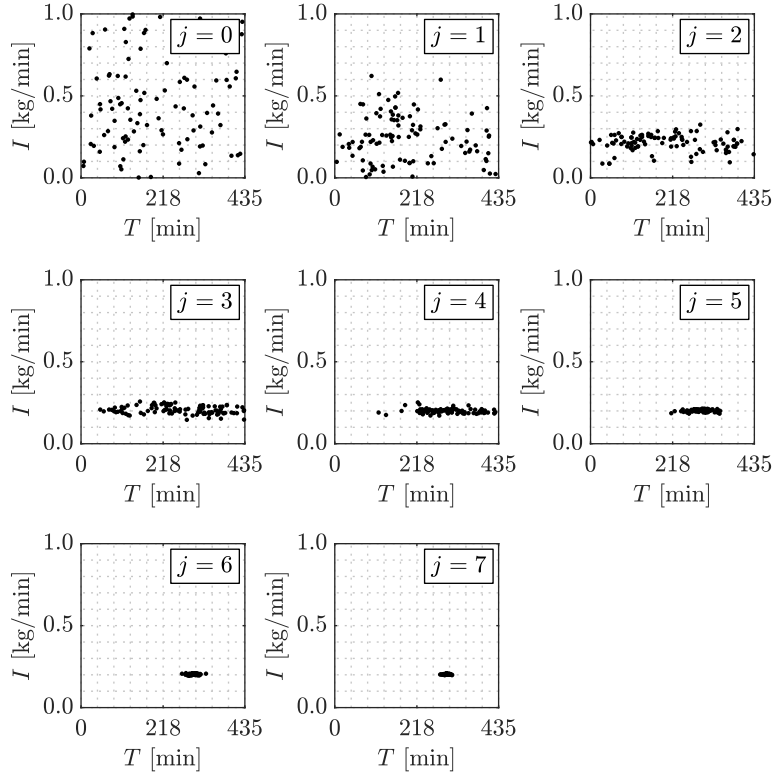


Figure 18: Plot of samples in the $T - I$ space generated at different steps of the transitional Markov chain Monte Carlo method when updating the model class associated with node 157. Application problem. Event 2

5.2.5. Computational cost

The proposed approach presents advantageous features for implementation in a high performance computing environment. As previously pointed out, the computational burden is almost entirely associated with the water quality analyses of the water distribution network. The number of network simulation runs for each model class depends, among other things, on the amount of samples per stage and the number of TMCMC stages needed. In Event 2, the computational effort for obtaining one water network solution is approximately 0.43 s and the average time spent to obtain posterior samples of a given model class is about 6.4 min. Considering a parallel implementation to evaluate the evidences of the model classes and neglecting the generation of posterior samples, which are not required by the evidence estimate provided by the TMCMC method, the entire model class selection process takes about 1.3 hrs. The previous computational efforts are based on the implementation of the identification process in available twelve-core multi-threaded computer units. Of course, if more

advanced computer power is available, the time to solve the contaminant source characterization problem can be significantly reduced.

6. Conclusions

A Bayesian model class selection framework for handling contaminant source characterization problems in the context of water distribution networks has been presented. The parameters of each model class characterize the contaminant mass inflow over time in terms of its intensity and starting time. The class with the highest posterior probability is interpreted as the most plausible location for the contaminant injection. The evidences of the model classes are estimated as a by-product of the model updating technique, i.e., the transitional Markov chain Monte Carlo method. The model updating technique is combined with a multi-purpose hydraulic and water quality simulation model in order to obtain the quantities of interest, including concentration measurements at a number of nodes. In addition, the proposed methodology presents advantageous features for its implementation in a high performance computing environment.

The effectiveness and capabilities of the proposed methodology are demonstrated with a couple of water distribution systems. Results indicate that overall, the proposed method is potentially a useful tool to address contaminant source detection problems. The proposed approach can provide relevant information for decision making processes even when relatively scarce and noisy data are available. In addition, it can provide additional insight into the actual system state in terms of the characteristics of the injection process. Generally, the scenarios where the actual injection node was not identified are associated with high levels of uncertainty and relatively short measurements periods. However, in these cases, the method is still able to identify nodes that are close to the actual source. The results also show the importance of an appropriate selection of the sensors configuration in order to improve the accuracy of contaminant source detection and therefore the safety of water utility networks.

Future research efforts involve the assessment of the proposed technique in more complex water

distribution networks and the consideration of field data as well as multiple sources of contamination and alternative injection profiles. The implementation of optimal sensor location strategies to improve the predictive capability of the proposed approach in the framework of utility networks is an additional subject for future research. Another research direction is the treatment of binary or fuzzy sensors as well as the integration of pre-screening techniques and surrogate models within the proposed framework. Finally, the consideration of stochastic models such as water-demand models within the proposed identification scheme is also one topic for further research. Some of these issues are currently under consideration.

Acknowledgments

The research reported here was supported in part by CONICYT (National Commission for Scientific and Technological Research) under grant number 1200087. Also, this research has been supported by CONICYT and DAAD under CONICYT-PFCHA/Doctorado Acuerdo Bilateral DAAD Becas Chile/2018-62180007. In addition, this research has been partially supported by DFG (German Research Foundation) under Grant No.BE 2570/3-1 and BR 5446/1-1. These supports are gratefully acknowledged by the authors.

7. Appendix

The following pseudo-code illustrates the implementation of the transitional Markov chain Monte Carlo method [31] to obtain posterior samples associated with the i^{th} model class M_i . It is assumed that the corresponding log-likelihood function $\mathcal{L}_i(\boldsymbol{\theta}_i) = \ln(p(D|M_i, \boldsymbol{\theta}_i))$ is available (see Eq. (5)).

1. Define β^2 . Set $j = 0$ and $\alpha_0 = 0$. Obtain samples $\boldsymbol{\theta}_{i,j}^k, k = 1, \dots, N_0$, distributed according to the prior distribution $p(\boldsymbol{\theta}_i|M_i)$. Compute the corresponding log-likelihood values $\mathcal{L}_{i,j}^k = \mathcal{L}_i(\boldsymbol{\theta}_{i,j}^k), k = 1, \dots, N_0$. Note that this step is equivalent to perform direct Monte Carlo simulation.

2. Define $\mathcal{L}^* = \max_{k=1, \dots, N_j} \mathcal{L}_{i,j}^k$. Compute α^* such that

$$\frac{\sigma_w}{\mu_w} = 1 \quad (9)$$

where

$$\mu_w = \frac{1}{N_j} \sum_{k=1}^{N_j} \exp \{(\alpha^* - \alpha_j)(\mathcal{L}_{i,j}^k - \mathcal{L}^*)\} \quad (10)$$

$$\sigma_w = \sqrt{\frac{1}{N_j - 1} \sum_{k=1}^{N_j} (\exp \{(\alpha^* - \alpha_j)(\mathcal{L}_{i,j}^k - \mathcal{L}^*)\} - \mu_w)^2} \quad (11)$$

3. Set $\alpha_{j+1} = \min(1, \alpha^*)$ and compute

$$\hat{w}_{i,j}^k = \exp \{(\alpha_{j+1} - \alpha_j)(\mathcal{L}_{i,j}^k - \mathcal{L}^*)\} \quad (12)$$

$$\bar{w}_{i,j}^k = \frac{\hat{w}_{i,j}^k}{\sum_{\iota=1}^{N_j} \hat{w}_{i,j}^\iota} \quad (13)$$

$$\ln(W_{i,j}) = \ln \left(\frac{1}{N_j} \sum_{k=1}^{N_j} \hat{w}_{i,j}^k \right) + (\alpha_{j+1} - \alpha_j) \mathcal{L}^* \quad (14)$$

4. If $\alpha_{j+1} = 1$ and no posterior samples are required, go to step 8. Otherwise, continue with step 5.

5. Obtain the parameters of the proposal distribution

$$\bar{\theta}_{i,j} = \sum_{k=1}^{N_j} \bar{w}_{i,j}^k \theta_{i,j}^k \quad (15)$$

$$\Sigma_{i,j} = \beta^2 \sum_{k=1}^{N_j} \bar{w}_{i,j}^k (\theta_{i,j}^k - \bar{\theta}_{i,j}) (\theta_{i,j}^k - \bar{\theta}_{i,j})^T \quad (16)$$

and define $\theta_{i,j}^{k(\text{loc})} = \theta_{i,j}^k, k = 1, \dots, N_j$, and $\mathcal{L}_{i,j}^{k(\text{loc})} = \mathcal{L}_{i,j}^k, k = 1, \dots, N_j$. These variables are used to track the evolution of each Markov chain.

6. Apply the Metropolis-Hastings algorithm [46, 47] to generate N_{j+1} samples distributed according to $p_{j+1}(\boldsymbol{\theta}_i) \propto p(\boldsymbol{\theta}_i|M_i)p(D|M_i, \boldsymbol{\theta}_i)^{\alpha_{j+1}}$. For $k = 1$ to N_{j+1} :

- (a) Draw ν from the set $\{1, 2, \dots, N_j\}$ with probabilities equal to the normalized weights $\bar{w}_{i,j}^\nu, \nu = 1, \dots, N_j$. Set the lead sample as $\boldsymbol{\theta}_i^{\text{lead}} = \boldsymbol{\theta}_{i,j}^{\nu(\text{loc})}$ with $\mathcal{L}_i^{\text{lead}} = \mathcal{L}_{i,j}^{\nu(\text{loc})}$.
- (b) Generate a candidate sample $\boldsymbol{\theta}_i^{\text{cand}}$ from a multivariate normal distribution with covariance matrix $\Sigma_{i,j}$ and centred at $\boldsymbol{\theta}_i^{\text{lead}}$. If $p(\boldsymbol{\theta}_i^{\text{cand}}|M_i) = 0$, set $\Upsilon = 1$ and go to Step 5-(c). Otherwise, compute $\mathcal{L}_i^{\text{cand}} = \mathcal{L}_i(\boldsymbol{\theta}_i^{\text{cand}})$ and

$$\ln(\Upsilon) = \alpha_{j+1} (\mathcal{L}_i^{\text{cand}} - \mathcal{L}_i^{\text{lead}}) + \ln(p(\boldsymbol{\theta}_i^{\text{cand}}|M_i)) - \ln(p(\boldsymbol{\theta}_i^{\text{lead}}|M_i)) \quad (17)$$

- (c) Generate ξ uniformly distributed on $[0, 1]$. If $\ln(\xi) \leq \min\{\ln(\Upsilon), 0\}$, set $\boldsymbol{\theta}_{i,j+1}^k = \boldsymbol{\theta}_i^{\text{cand}}$, $\mathcal{L}_{i,j+1}^k = \mathcal{L}_i^{\text{cand}}$ and update the last element of the current Markov chain as $\boldsymbol{\theta}_{i,j}^{\nu(\text{loc})} = \boldsymbol{\theta}_i^{\text{cand}}$ and $\mathcal{L}_{i,j}^{\nu(\text{loc})} = \mathcal{L}_i^{\text{cand}}$. Otherwise, set $\boldsymbol{\theta}_{i,j+1}^k = \boldsymbol{\theta}_i^{\text{lead}}$ and $\mathcal{L}_{i,j+1}^k = \mathcal{L}_i^{\text{lead}}$.

7. If $\alpha_{j+1} < 1$, set $j \leftarrow j + 1$ and go back to step 2. Otherwise, continue with step 8.

8. Stop the sampling process, set $m = j + 1$, and compute the evidence estimate as

$$P(D|M_i) \approx W_i = \exp\left(\sum_{j=0}^{m-1} \ln(W_{i,j})\right) \quad (18)$$

References

References

- [1] World Health Organization. Guidelines for drinking-water quality. Geneva, Switzerland, 2017.
- [2] M.-C. Besner, M. Prévost, and S. Regli. Assessing the public health risk of microbial intrusion events in distribution systems: Conceptual model, available data and challenges. *Water Research*, 45(3):961–183, 1996.

- [3] R. Janke, M. E. Tryby, and R. M. Clark. Protecting water supply critical infrastructure: An overview. *Securing Water and Wastewater Systems*, 29–85. Springer International Publishing, 2013.
- [4] E. Z. Berglund, J. E. Pesantez, A. Rasekh, M. E. Shafiee, L. Sela, and T. Haxton. Review of modeling methodologies for managing water distribution security. *Journal of Water Resources Planning and Management*, 146(8):03120001, 2020.
- [5] J. Guan, M. M. Aral, M. L. Maslia, and W. M. Grayman. Identification of contaminant sources in water distribution systems Using Simulation-optimization method: case study. *Journal of Water Resources Planning and Management*, 132(4):252–262, 2006.
- [6] A. Preis and A. Ostfeld. A contamination source identification model for water distribution system security. *Engineering Optimization*, 39(8):941–947, 2007.
- [7] C. L. Laird, L. T. Biegler, B. G. van Bloemen Waanders, and R. A. Bartlett. Contamination source determination for water distribution networks. *Journal of Water Resources Planning and Management*, 131(2):125–134, 2005.
- [8] A. Preis and A. Ostfeld. Genetic algorithm for contaminant source characterization using imperfect sensors. *Civil Engineering and Environmental Systems*, 25(1):29–39, 2008.
- [9] A. E. De Sanctis, F. Shang, and J.G. Uber. Real-time identification of possible contamination sources using network backtracking methods. *Journal of Water Resources Planning and Management*, 136(4):444–453, 2010.
- [10] L. Liu, S. R. Ranjithan, and G. Mahinthakumar. Contamination source identification in water distribution systems using an adaptive dynamic optimization procedure. *Journal of Water Resources Planning and Management*, 137(2):183–192, 2011.
- [11] J. Kumar, E. D. Brill, G. Mahinthakumar, and S. R. Ranjithan. Contaminant source characterization in water distribution systems using binary signals. *Journal of Hydroinformatics*, 14(3):585–602, 2012.
- [12] D. M. Costa, L. F. Melo, and F. G. Martins. Localization of contamination sources in drinking water distribution systems: A method based on successive positive readings of sensors. *Water*

Resources Management, 27(13):4623–4635, 2013.

- [13] H. Shen and E. McBean. False negative/positive issues in contaminant source identification for water-distribution systems. *Journal of Water Resources Planning and Management*, 138(3):230–236, 2012.
- [14] L. Grbčić, I. Lučin, L. Kranjčević, and S. Družeta. A Machine Learning-based algorithm for water network contamination source localization. *Sensors*, 20(9):2613, 2020.
- [15] E. J. M. Blokker, J. H. G. Vreeburg, and J. C. van Dijk. Simulating residential water demand with a stochastic end-use model. *Journal of Water Resources Planning and Management*, 136(1):19–26, 2010.
- [16] Y. Bao and L. W. Mays. Model for water distribution system reliability. *Journal of Hydraulic Engineering*, 116(9):1119–1137, 1990.
- [17] CNIP’06. *Proceedings of the International Workshop on Complex Network and Infrastructure Protection*. Rome, Italy, 2006.
- [18] E. T. Jaynes. *Probability theory: The logic of science*. Cambridge University Press, Cambridge, 2003.
- [19] E. Ortega, A. Braunstein, and A. Lage-Castellanos. Contamination source detection in water distribution networks using belief propagation. *Stochastic Environmental Research and Risk Assessment*, 34(3-4):493–511, 2020.
- [20] X. Yang and D. L. Boccelli. Bayesian approach for real-time probabilistic contamination source identification. *Journal of Water Resources Planning and Management*, 140(8):04014019, 2014.
- [21] N. Sankary and A. Ostfeld. Bayesian localization of water distribution system contamination intrusion events using inline mobile sensor data. *Journal of Water Resources Planning and Management*, 145(8):04019029, 2019.
- [22] R. M. Neupauer, M. K. Records, and W. H. Ashwood. Backward probabilistic modeling to identify contaminant sources in water distribution systems. *Journal of Water Resources Planning and Management*, 136(5):587–591, 2010.
- [23] L. Perelman and A. Ostfeld. Bayesian networks for source intrusion detection. *Journal of Water*

Resources Planning and Management, 139(4):426–432, 2013.

- [24] W. J. Dawsey, B. S. Minsker, and V. L. VanBlaricum. Bayesian belief networks to integrate monitoring evidence of water distribution system contamination. *Journal of Water Resources Planning and Management*, 132(4):234–241, 2006.
- [25] H. Wang and K. W. Harrison. Bayesian update method for contaminant source characterization in water distribution systems. *Journal of Water Resources Planning and Management*, 139(1):13–22, 2013.
- [26] H. Wang and K. W. Harrison. Bayesian update method for contaminant source characterization in water distribution systems. *Stochastic Environmental Research and Risk Assessment*, 27(8):1921–1928, 2013.
- [27] H. Wang and K. W. Harrison. Improving efficiency of the Bayesian approach to water distribution contaminant source characterization with support vector regression. *Journal of Water Resources Planning and Management*, 140(1):3–11, 2014.
- [28] J. Beck and L. Katafygiotis. Updating models and their uncertainties. I: Bayesian statistical framework. *Journal of Engineering Mechanics*, 124(4):455–461, 1998.
- [29] L. Katafygiotis and J. Beck. Updating models and their uncertainties. II: Model Identifiability. *Journal of Engineering Mechanics*, 124(4):463–467, 1998.
- [30] K. V. Yuen. *Bayesian methods for structural dynamics and civil engineering*, John Wiley & Sons. 2010.
- [31] J. Ching and Y.C. Chen. Transitional Markov chain Monte Carlo method for Bayesian updating, model class selection, and model averaging. *Journal of Engineering Mechanics*, 133:816–832, 2007.
- [32] H. A. Jensen and D. J. Jerez. A Bayesian model updating approach for detection-related problems in water distribution networks. *Reliability Engineering and System Safety*, 185:100–112, 2019.
- [33] L. A. Rossman, H. Woo, M. Tryby, F. Shang, R. Janke, and T. Haxton. *EPANET 2.2 User Manual*. U.S. Environmental Protection Agency, Cincinnati, Ohio, 2020.

- [34] D. G. Eliades, M. Kyriakou, S. Vrachimis, and M. M. Polycarpou. EPANET-MATLAB Toolkit: An open-source software for interfacing EPANET with MATLAB. *Proceedings of the 14th International Conference on Computing and Control for the Water Industry (CCWI)*, 2016.
- [35] L. Liu and A. Sankarasubramanian and S. R. Ranjithan. Logistic regression analysis to estimate contaminant sources in water distribution systems. *Journal of Hydroinformatics*, 13(3):545–557, 2010.
- [36] C. Di Cristo and L. Leopardi. Pollution source identification of accidental contamination in water distribution networks. *Journal of Water Resources Planning and Management*, 134(2):197–202, 2008.
- [37] D.E. Goldberg. Genetic algorithms in search, optimization and machine learning, *Addison-Wesley*, Reading,MA. 1999.
- [38] T.H. Holland. Adaptation in natural and artificial systems, *University of Michigan Press*, Ann Arbor, Michigan, 1975.
- [39] S. Kirkpatrick, C.D. Gelatt, M.P. Vecchi. Optimization by simulated annealing, *Science*, 220(4589):165–172, 1983.
- [40] J.C. Spall Introduction to stochastic search and optimization: estimation, simulation, and control, *John Wiley and Sons*, New York, 2003.
- [41] J. L. Beck. Bayesian system identification based on probability logic. *Structural Control and Health Monitoring*, 17(7):825–847, 2010.
- [42] H. A. Jensen and D. J. Jerez. A stochastic framework for hydraulic performance assessment of complex water distribution networks: Application to connectivity detection problems. *Probabilistic Engineering Mechanics*, 60:103029, 2020.
- [43] J. L. Beck and K. V. Yuen. Model selection using response measurements: Bayesian probabilistic approach. *Journal of Engineering Mechanics*, 130(2):192–203, 2004.
- [44] A. Kong, J. S. Liu, and W. H. Wong. Sequential imputations and Bayesian missing data problems. *Journal of the American Statistical Association*, 89(425):278–288, 1994.
- [45] J. S. Liu. Metropolized independent sampling with comparisons to rejection sampling and

- importance sampling. *Statistics and Computing*, 6(2):113–119, 1996.
- [46] N. Metropolis, A. Resenbluth, M. Resenbluth, A. Teller, and E. Teller. Equations of state calculations by fast computing machines. *Journal of Chemical Physics*, 21(6):1087–1092, 1953.
- [47] W. Hastings. Monte Carlo sampling methods using Markov chains and their applications. *Biometrika*, 57(1):97–109, 1970.
- [48] W. Betz, I. Papaioannou, and D. Straub. Transitional Markov Chain Monte Carlo: Observations and improvements. *Journal of Engineering Mechanics*, 142(5), 2016.
- [49] H. A. Jensen, C. Esse, V. Araya, and C. Papadimitriou. Implementation of an adaptive meta-model for Bayesian finite element model updating in time domain. *Reliability Engineering and System Safety*, 160:174–190, 2016.
- [50] P. Angelikopoulos, C. Papadimitriou, and P. Koumoutsakos. X-TMCMC: Adaptive kriging for Bayesian inverse modeling. *Computer Methods in Applied Mechanics and Engineering*, 289:409–428, 2015.
- [51] L. S. Katafygiotis, O. Sedehi, and F. R. Rofooei. Bayesian time-domain model updating considering correlation of prediction errors. *12th International Conference on Structural Safety and Reliability* Vienna, Austria, 2017.
- [52] E. Simoen, C. Papadimitriou, and G. Lombaert. On prediction error correlation in Bayesian model updating. *Journal of Sound and Vibration*, 332(18), 4136–4152, 2013.
- [53] M. F. Pellissetti. Parallel processing in structural reliability. *Journal of Structural Engineering and Mechanics*, 32(1):95–126, 2009.
- [54] Z. Poulakis, D. Valougeorgis, and C. Papadimitriou. Leakage detection in water pipe networks using a Bayesian probabilistic framework. *Probabilistic Engineering Mechanics*, 18(4):315–327, 2003.
- [55] J. Berry, et al. *User’s manual: TEVA-SPOT toolkit 2.4..* EPA 600/R-08/041B, National Homeland Security Research Center, U.S. EPA, Washington, 2010.